

Medical Aegis: Robust adversarial protectors for medical images

Qingsong Yao
ICT, CAS

yaoqingsong19@mailsucas.edu.cn

Zecheng He
Princeton University

zechengh@princeton.edu

Shaohua Kevin Zhou
USTA & ICT, CAS

zhoushaohua@ict.ac.cn

Abstract

Deep neural network based medical image systems are vulnerable to adversarial examples. Many defense mechanisms have been proposed in the literature, however, the existing defenses assume a passive attacker who knows little about the defense system and does not change the attack strategy according to the defense. Recent works [2, 3, 52] have shown that a strong adaptive attack, where an attacker is assumed to have full knowledge about the defense system, can easily bypass the existing defenses. In this paper, we propose a novel adversarial example defense system called *Medical Aegis*. To the best of our knowledge, *Medical Aegis* is the first defense in the literature that successfully addresses the strong adaptive adversarial example attacks to medical images. *Medical Aegis* boasts two-tier protectors: The first tier of *Cushion* weakens the adversarial manipulation capability of an attack by removing its high-frequency components, yet posing a minimal effect on classification performance of the original image; the second tier of *Shield* learns a set of per-class DNN models to predict the logits of the protected model. Deviation from the *Shield*'s prediction indicates adversarial examples. *Shield* is inspired by the observations in our stress tests that there exist robust trails in the shallow layers of a DNN model, which the adaptive attacks can hardly destruct. Experimental results show that the proposed defense accurately detects adaptive attacks, with negligible overhead for model inference.

1. Introduction

It is celebrated that deep neural networks (DNNs) are vulnerable to adversarial attacks [50]. These notorious attacks maliciously force the network to generate attacker-desired incorrect predictions by adding human-imperceptible perturbations to clean examples [11]. This defect limits DNNs to be further applied in many security-critical applications, including autonomous driving [13] and face recognition [44]. Especially, for medical imaging, the adversarial attack is disastrous for its ability to manipulate patients' disease diagnosis and disturb the subsequent

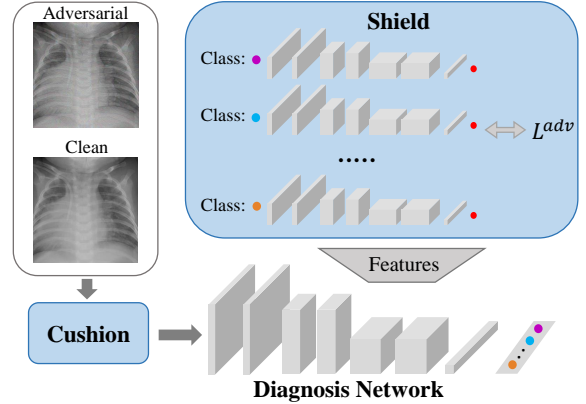


Figure 1. The overall framework of *Medical Aegis*, which is a cascade consisting of a *Cushion* and a *Shield*. The *Cushion* removes the high-frequency components and weakens the adversarial attacks, while the *Shield* consists of adversarial detectors for each class. The detector takes the feature of both shallow and deep layers from the pretrained diagnosis network as input and is adversarially trained by adaptive attacks.

treatment. Sadly, the attacker is proved to compromise the DNNs for medical images more easily than natural images in multiple tasks, including organ segmentation [7, 40], disease diagnosis [17, 45], and landmark detection [57].

The above threats raise an urgent need for advanced approaches to help DNNs make robust decisions. Blooming defenses have been developed to alleviate adversarial attacks, which are broadly categorized into two classes: *proactive* and *reactive*. Adversarial training [53], as one of the most representative proactive defenses with the highest robustness [10], sacrifices the model performances [54] and consumes the training time [48]. More disturbingly, other proactive defenses like input transformation [19] have a limited power of removing adversarial perturbations and can be bypassed by the adaptive attacks [2, 3, 52].

Another mainstream of defenses is reactive defense, which aims at detecting adversarial examples and purging them. The reactive defense has two significant advantages. On the one hand, adversarial detectors can be easily de-

ployed to protect a pretrained DNN without sacrificing performance or retraining the model. On the other hand, recent studies [5, 8] have shown the great potential of reactive defense to recognize adversarial examples with nearly 100% accuracy.

However, the reactive defenses in the literature, though having the aforementioned advantages for natural images, can hardly work for medical images. Ma *et al.* [34] discover that the great vulnerability of medical image comes from the vulnerability of deep representations. The attacker can easily control the prediction by drastically changing the features. Naturally, anomaly detection approaches are deployed to identify these adversarial features which are out of the normal distributions [28, 34] to defend against the conventional attacks. However, once the attackers are aware of this defense strategy, they can utilize the vulnerability of features to better imitate the normal features. Yao *et al.* [58] boost the conventional attacks, resulting in *adaptive attacks* with hierarchical feature constraint (HFC) to completely bypass a fleet of detectors. Defeating these **adaptive attacks, where the attacker has full knowledge about the defense mechanism**, remains a challenging and unsolved problem.

By analyzing the evolving arm race between the attacker and detector, we observe that the vulnerability of medical features is the key to empowering the attacker to bypass both diagnosis networks and adversarial detectors. However, as constrained by the perturbation intensity, there is a limit to the manipulative capability of the adaptive attack. To confirm this, we perform the same stress test designed in [58] on features from different layers to quantify this capability, which aims to distort the features by the adversarial attack. The results show that shallow features are more robust than deep ones, which encourages more exploitation of the shallow layers in reactive defenses.

In this paper, we assume a strong attacker who is aware of the details about the defense, *i.e.*, adaptive attacks. Our goal is to protect the medical image models from various conventional and adaptive adversarial attacks. *Firstly*, we propose Cushion, which weakens the adversarial examples to arbitrarily manipulate the medical features by removing the high-frequency components, but with a minimum impact on the original image. *Then*, once the learning-based detector is aware that the attacker deploys adaptive attacks such as HFC [57], the detectors can also improve the robustness by fine-tuning on the adversarial examples generated by adaptive attacks. The confrontation evolves into adversarial training. The detector aims at finding more unique characteristics of the adversarial features distinguishable from the normal ones, especially in the shallow layers. On the opposite side, the adaptive attack tries to destruct these trails, and mimics clean features in the feature space. Thus, the adversarial training on deep representations re-

sults in a robust detector, which we name as Shield. Inspired by [16, 26, 59], we train a separate DNN model as the adversarial detector for each class. As shown in Fig. 1, after the protected diagnosis network makes the decision, the features are sent to the corresponding detector. *Finally*, we deploy “Cushion” to help the adversarial detectors in “Shield” win the combat more easily by weakening the adversarial attacks, resulting in a novel two-tier defense system called Medical Aegis.

We summarize the key contributions as follows:

- We perform stress tests to quantitatively evaluate the manipulative capability of adversarial examples to manipulate the vulnerable medical features of different layers. Furthermore, we observe that there exist robust trails in the shallow layers of a DNN model, which the adaptive attacks can hardly destruct.
- We propose Cushion, which weakens the adversarial examples to arbitrarily manipulate the medical features and strengthens a set of adversarial detectors against adaptive attacks. We also propose Shield, which spots the manipulative trails, especially in the shallow feature layers through adversarial learning.
- We propose a novel, two-tier defense system, *i.e.*, Medical Aegis, against adversarial example attacks. Medical Aegis, formed by an integration of Cushion and Shield, is the first defense that successfully addresses strong adaptive attacks, where an attacker has full knowledge about the defense.
- We systematically evaluate our proposed defense on two benchmark medical image datasets, with different deep network backbones, and against both conventional and adaptive attacks to demonstrate the effectiveness of Medical Aegis in protecting a pertained medical image diagnosis network.

The rest of the paper is organized as follows: Section 2 introduces the background and related work of adversarial example attacks and defenses. Section 3 presents our proposed Cushion, Shield, and Medical Aegis system. We provide the experimental details in Section 4 to show the effectiveness of the design. We conclude the work and discuss potential future work directions in Section 5.

2. Related Work

Preliminaries. Given a clean image x with its ground truth label $y \in [1, 2, \dots, Y]$ and a DNN classifier h with pretrained parameters θ , the classifier predicts the class of the input example y' via:

$$y' = \arg \max_c h_{\theta}^c(x) \equiv \frac{\exp(l_{\theta}^c(x))}{\sum_{j=1}^Y \exp(l_{\theta}^j(x))}. \quad (1)$$

where $l_{\theta}^c(x)$ is the logits output and the $h_{\theta}^x(x)$ is the posterior probability of x belonging to class c .

2.1. Adversarial attacks

Conventional white-box adversarial attacks generate adversarial examples by minimizing¹ the classification error between the prediction and target class c , while keeping the adversarial example x_{adv} within a small ϵ -ball of the L_p -norm [35] centered at the clean sample x , i.e., $\|x_{adv} - x\|_p \leq \epsilon$, where ϵ is perturbation budget.

These attack methods can be roughly divided into two categories. The first category is gradient-based approaches [12, 55], such as fast gradient sign method (FGSM) [18], basic iterative method (BIM) [25], momentum iterative method (MIM) [11] and projected gradient descent (PGD) [35], which generates the adversarial example x^* by minimizing the loss $J(h_{\theta}^c(x^*))$, with J often chosen as the cross-entropy loss and ϵ the L_{∞} norm bound. A typical iteration proceeds as below:

$$x_{t+1}^* = \Pi_{\epsilon}(x_t^* - \alpha \cdot \text{sign}(\nabla_x J(h_{\theta}^c(x_t^*)))) \quad (2)$$

The second category is optimization-based methods. DeepFool [39] is an L_2 -norm attack method that moves the attacked input sample to its closest decision boundary. Furthermore, Carlini and Wagner propose the CW attack [4], which shows the greatest ability to bypass an array of neural networks and adversarial defenses [2, 3] with small perturbations. Especially, the L_{∞} version of CW attack can be solved by the PGD algorithm by using the following objective function:

$$J_{cw} = \max(l_{\theta}^c(x_t^*) - l_{\theta}^{y_{max} \neq c}(x_t^*), -\kappa) \quad (3)$$

where $l_{\theta}^{y_{max} \neq c}(\cdot)$ is the maximum logits of the remaining classes, and κ is a parameter managing the confidence.²

2.2. Adversarial defenses

A variety of *proactive defense* approaches have been proposed, such as feature squeezing [56], distillation network [43], input transformation (e.g., JPEG compression [15], total variation minimization [19], autoencoder-based denoising [29] and regularization [46]), randomization [9, 30], gradient masking [42], radial basis mapping kernel [51] and non-local context encoder [21]. Despite the success of these methods to defend conventional attacks, they still can be bypassed either partially or completely by adaptive attacks [2, 3, 52]. Another research line is adversarial (re)training [18, 35, 53], which augments the training set with adversarial examples and achieves the highest robustness among proactive defenses (according to [10]).

¹In this work, we focus on targeted adversarial attack.

²We set κ to the average difference between the largest logits and the penultimate logits for each dataset.

However, adversarial training not only consumes too much training and inference time [48], but also compromises the model performance [54].

On the contrary, *reactive defenses* protect the system by detecting the adversarial examples from clean images [36, 38]. In particular, several emerging works shed light on the intrinsic characteristic of the deep adversarial representations [8, 27, 60]. Some of them use learning-based approaches (e.g., RBF-SVM [32], DNN [37]) to develop a decision boundary between clean and adversarial examples in the high dimensional feature subspace. Another line of research is k-nearest neighbors (kNN) [1, 5, 14, 41] based methods, which focus on distinguishing adversarial examples based on their relationship to other clean images in the calibrated dataset. Furthermore, a family of anomaly-detection approaches [60] has been deployed to detect adversarial examples: Feinman et al. [16] model the clean distribution with kernel density estimation. Ma et al. [33] characterize the dimensional properties of the adversarial features by local intrinsic dimensionality. Lee et al. [26] measure the degree of the outlier by a Mahalanobis distance based confidence score.

Deviling into defenses against medical adversarial attacks, the aforementioned reactive approaches can identify *conventional attacks* with nearly 100% accuracy [28, 34], which benefits from the vulnerable medical features [58]. Unluckily, when facing *adaptive attacks*, the attacker can easily compromise these detectors by mimicking clean features with the help of hierarchical feature constraint [58] or feature attack [47]. In this work, we challenge to build robust protectors to *defeat the strongest adaptive attack*.

3. Method

In this section, we first perform a stress test to evaluate the vulnerability of the medical features in different layers of the diagnosis network. Then, we introduce ‘‘Cushion’’ in Section 3.1 and explore its potential to prevent the attacker from arbitrarily manipulating medical features. Next, we demonstrate the training strategy of ‘‘Shield’’ in Section 3.2. Finally, we demonstrate how ‘‘Medical Aegis’’ aggregates ‘‘Cushion’’ and ‘‘Shield’’ to detect medical adversarial examples in Section 3.3.

Given the fact concluded in [34, 58]: the vulnerable features of medical images make the diagnosis network and adversarial detectors more easily bypassed by conventional attacks [34] and adaptive attacks [58], compared to the natural images. A question arises naturally: *In the procedure of diagnosis network from taking image as input to generating final logits, what is the maximum capacity of the attacker to manipulate medical features from different layers?* We perform stress tests (designed in [58]) to evaluate the robustness of features from different layers and logits. Specifically, for features, we decrease (\downarrow) and increase

Table 1. Comparison of the vulnerability of the medical features from different layers, as well as using “Cushion” (JPEG compression [19] in this experiment) or not. We calculate the differences (diff.) of logits and the mean values of the features from different layers of ResNet-50. The relative changes of the values are reported in parentheses, bigger change indicates greater vulnerability. If “Cushion” is applied, the attacker equip BIM [25] with BPDA [2] accordingly. The stress test uses perturbations under the constraint $L_\infty = 4/256$.

Funduscopy	Number of residual block				Penultimate	Logits (Diff.)
	1 st	4 th	10 th	15 th		
Clean	.124(100%)	.101(100%)	.070(100%)	.233(100%)	.425(100%)	8.39(100%)
No JPEG (↑)	.133(+7.14%)	.133(+31.7%)	.123(+73.4%)	.720(+210%)	2.471(+481%)	40.52(+393%)
JPEG-90 (↑)	.124(+0.30%)	.115(+13.5%)	.090(+25.8%)	.449(+92.3%)	1.273(+199%)	23.63(+182%)
JPEG-70 (↑)	.124(-0.52%)	.106(+4.58%)	.075(+5.60%)	.302(+29.9%)	.654(+53.7%)	13.69(+63.1%)
No JPEG (↓)	.111(-10.9%)	.091(-9.78%)	.051(-28.1%)	.112(-51.8%)	.087(-79.4%)	1.45(-82.7%)
JPEG-90 (↓)	.113(-9.40%)	.097(-3.79%)	.059(-16.9%)	.132(-44.3%)	.103(-75.7%)	1.46(-82.6%)
JPEG-70 (↓)	.115(-7.80%)	.100(-0.69%)	.065(-8.99%)	.165(-29.2%)	.188(-55.7%)	4.01(-52.0%)

(↑) the features as much as possible by adversarial attacks. In implementation, we replace the loss function J in BIM (Eq. 2) by $J_\downarrow^* = \text{mean}(f_\theta^l(x))$ and $J_\uparrow^* = -\text{mean}(f_\theta^l(x))$, respectively, where $f_\theta^l(x)$ is the activation value from the l^{th} layer. For logits, we try decrease (↓) and increase (↑) the differences between the l^1 (logits of class 1, DR) and l^0 (logits of class 0, No DR)³. We replace J by $J_\downarrow^* = \text{abs}(l^1 - l^0)$ and $J_\uparrow^* = -\text{abs}(l^1 - l^0)$.

The comparison results shown in Table 1 demonstrate the following trait: adversarial attacks can alter the medical features from the deeper layers more drastically. Such a trait has both positive and negative implications. On the negative side, the adaptive attack can utilize this great vulnerability of deep features to compromise the detectors; on the positive side, it is possible to find some robust trails of the adversarial attacks, especially in the features of shallow layers, which the adaptive attacks can not destruct.

3.1. Cushion

We alleviate the adaptive attacks by leveraging a pre-processing step called “Cushion” denoted by \mathcal{C} , which removes high-frequency components of an input image. Essentially, it performs the act of denoising before sending it to the diagnosis network:

$$\hat{x} = C_\lambda(x), \quad (4)$$

where λ is the hyper-parameter controlling the denoising degree. In this paper, we choose JPEG compression [15, 19] as the “Cushion” protector \mathcal{C} , in which λ is the compression quality. In the ablation study, we investigate the Cushion choices too.

“Cushion” is inspired from the hypothesis proposed and validated in [22]: adversarial attacks compromise the DNNs

³We perform the stress test on the binary classification medical dataset (“Funduscopy”), where the images are categorized as “diabetic retinopathy (DR)” and “No DR”. Please see Section 4.1 for more detail.

by attributing the *non-robust* signals, which are brittle, of high-frequency, imperceptible and incomprehensible to humans. Despite that using denoising approaches alone can not defend against the adaptive attack equipped with Backward Pass Differentiable Approximation (BPDA) [2], we believe that removing some of the high-frequency and imperceptible signals can prevent the adaptive attacks from manipulating medical features. To evaluate our hypothesis, we continue to perform the stress test introduced above. Differently, we apply the “Cushion” operation before generating medical features, but still, we equip the attacker with BPDA.

As shown in Table 1, “Cushion” successfully reduces the attacker’s ability to manipulate medical features. Also, stronger denoising brings more robustness of medical deep representations, which is exactly what we need.

Algorithm 1 Training procedure of Medical Aegis

Input:

- Training set $(x^i, y^i) \in \mathcal{D}$, pretrained classifier h
- 1: **for** each class $y = 0$ to Y **do**
 - 2: **repeat**
 - 3: Sample x from \mathcal{D} with class y
 - 4: Sample \hat{x} from \mathcal{D} with class is not y
 - 5: Craft adversarial examples $f_\theta(\hat{x}_m^*)$ by optimizing (7) using PGD [35] equipped with BPDA [2]
 - 6: Train detector \mathcal{S} with the loss function L_m^{adv} in (8)
 - 7: **until** \mathcal{S} converges
 - 8: **end for**
 - 9: **return** Adversarial detectors \mathcal{S} for Y classes
-

3.2. Shield

We consider a white-box confrontation between the adversarial detectors and adaptive attacks, where both sides are fully aware of the opponent’s strategy and parameters. The detector is trained to identify adversarial examples gen-

Table 2. The performance of detectors against adversarial attacks is boosted with hierarchical feature constraint (HFC). When evaluating “Cushion” to strengthen the detectors, we implement strong adversarial attacks equipping BPDA [2]. All of the adversarial examples are generated under the constraint $L_\infty = 16/256$ on the funduscopy dataset. We use ResNet-50 as the backbone.

Funduscopy	MIM		BIM		PGD		CW- l_∞	
	AUROC	TPR@90	AUROC	TPR@90	AUROC	TPR@90	AUROC	TPR@90
KD	50.3	0.9	46.9	1.4	57.5	0.5	46.2	0.8
KD w/ Cushion	75.8	9.3	71.1	6.9	75.9	10.7	81.1	15.8
MAHA	1.2	0.0	0.7	0.0	5.2	0.0	0.7	0.0
MAHA w/ Cushion	80.7	3.7	75.1	16.3	82.0	24.7	83.2	26.0
LID	79.9	30.6	76.0	27.1	82.8	43.5	71.8	20.0
LID w/ Cushion	87.6	64.4	89.6	68.1	88.0	69.3	84.8	51.6
DNN	55.6	18.1	56.5	29.4	58.8	33.8	45.1	0.9
DNN w/ Cushion	89.3	79.1	67.9	49.3	71.9	55.8	89.8	85.6
Shield	99.0	97.7	99.0	97.6	99.2	97.8	98.9	97.2
Medical Aegis	100	100	100	100	100	100	100	100

erated by adaptive attacks in feature space, while the adaptive attack tries to bypass the detector by directly reducing their prediction scores in gradient back-propagation. Naturally, we perform *adversarial training in the feature space* to see which side can finally win this arm race.

Specifically, given the input image x , the pretrained classifier $h_\theta(x)$ first predicts the class y and records the features $f_\theta(x)$ of *from shallow to deep layers* at the same time, which presents a stark contrast with existing defense approaches that mostly exploit deep features. Then, for each class $y \in [1, 2, \dots, Y]$, we deploy a separate DNN-based detector \mathcal{S} with parameter ϕ that takes the features $f_\theta(x)$ ⁴ as input and predicts the logit $S_\phi[f_\theta(x)]$ and the probability $\sigma(S_\phi[f_\theta(x)])$ of clean example, where $\sigma(\cdot)$ denotes the sigmoid function.

In the training phase of the detector \mathcal{S} , the attacker samples \hat{x} from other classes and tries to bypass \mathcal{S} by increasing the logit $S_\phi[f_\theta(x)]$. In practice, we use L_∞ PGD [35] to generate adversarial examples \hat{x}_s^* by iteratively optimizing the following loss function:

$$J_{shield}(x) = -S_\phi[f_\theta(x)]. \quad (5)$$

For the detector \mathcal{S} , the adversarial loss L_s^{adv} is defined as follows:

$$L_s^{adv} = \log\{\sigma(S_\phi[f_\theta(x)])\} + \log\{1 - \sigma(S_\phi[f_\theta(\hat{x}_s^*)])\}. \quad (6)$$

Optimized by L_s^{adv} , the detectors distinguish clean features $f_\theta(x)$ (of the class y) from various adversarial features $f_\theta(\hat{x}_s^*)$. As demonstrated in Table 1, the adversarial attacks have limited power to manipulate the shallower features. As a consequence, detectors can learn a tight decision boundary around the robust clean features, which the

⁴Details can be found in 4.1.

attackers are hard to mimic. Therefore, we name the robust, adversarially-trained detector as “Shield”.

In the inference stage, the classifier predicts the class y of the input x and sends the features to the corresponding detector \mathcal{S} , which decides to accept according to the logit $S_\phi[f_\theta(x)]$.

3.3. Medical Aegis

As concluded in Section 3.1, the “Cushion” can effectively weaken the adaptive attacks by removing the high-frequency components in the input image, which can strengthen the “Shield” to win the confrontation against adaptive attacks more easily. In this section, we aggregate the advantages of “Cushion” and “Shield” in one defending system called “Medical Aegis”, which protects medical images against adversarial attacks.

In particular, for each input image x , we first use “Cushion” to smooth x . Then we predict the smoothed image $C_\lambda(x)$ as label y by classifier h with feature $f_\theta(C_\lambda(x))$. Next, we generate the logit $S_\phi[f_\theta(C_\lambda(x))]$ before feeding it to the detector \mathcal{S} . In the training stage, attacker crafts adversarial examples $f_\theta(\hat{x}_m^*)$ by optimizing the following object function using PGD [35] equipped with BPDA [2]:

$$J_{m.aegis}(x) = -S_\phi[f_\theta(C_\lambda(x))]. \quad (7)$$

For the detector \mathcal{S} , the adversarial loss L_s^{adv} is defined accordingly:

$$L_m^{adv} = \log\{\sigma(S_\phi[f_\theta(C_\lambda(x))])\} + \log\{1 - \sigma(S_\phi[f_\theta(C_\lambda(\hat{x}_m^*)])\}. \quad (8)$$

The inference stage is similar to “Shield” except for using “Cushion” in the first stage, and the final logit is computed as $S_\phi[f_\theta(C_\lambda(x))]$.

Table 3. The performances of “Shield” and “Medical Aegis” against an array of **conventional attacks** on different datasets and backbones. When we deploy “Cushion” as a pre-processing step, the adversarial attack will automatically equip BPDA [2]. The adversarial examples are under the constrain $L_\infty = 16/256$ or $L_2 = 8/256$. AUC scores (%) are used as metrics.

Fundoscopy	Defends	FGSM	BIM	PGD	MIM	DIM	TIM	CW- l_∞	PGD- l_2	CW	TF
ResNet-50	Shield	98.8	99.3	99.2	99.3	99.3	98.6	98.8	98.4	97.7	98.0
	Medical Aegis	100	100	100	100	100	99.9	99.8	99.8	92.3	100
VGG-16	Shield	99.8	99.8	99.7	99.8	99.8	98.7	98.5	97.9	97.0	99.7
	Medical Aegis	100	100	100	100	100	100	99.9	99.9	93.6	100
Chest X-Ray	Defends	FGSM	BIM	PGD	MIM	DIM	TIM	CW- l_∞	PGD- l_2	CW	TF
ResNet-50	Shield	89.5	98.1	98.1	98.3	98.0	97.9	97.5	97.2	96.7	97.8
	Medical Aegis	100	100	100	100	100	100	100	100	100	100
VGG-16	Shield	100	99.9	99.9	99.9	99.9	99.6	99.0	98.8	98.5	99.9
	Medical Aegis	100	100	100	100	100	100	100	99.6	98.6	100

4. Experiments

In this section, we first verify the effectiveness of the “Cushion” to help improve the performances of the state-of-the-art adversarial detectors in Section 3.1. Then, we evaluate “Medical Aegis” on different datasets and backbones against plenty of conventional and adaptive attacks in Section 3.3. Finally, to better understand the advantages and limitation of “Medical Aegis”, we test different models by extracting features from different layers, changing different “Cushions”, and using different perturbation constraints in Section 4.4.

4.1. Setup

Datasets. Following the literature [17, 33, 58], we use two representative public datasets on medical classification tasks. The first one is Kaggle Fundoscopy dataset [23] on the diabetic retinopathy (DR) classification task, consisting of 3,663 high-resolution fundus images. Each image is labeled to one of the five levels from ‘No DR’ to ‘mid/moderate/severe/proliferate DR’. Following [17, 34], we conduct a binary classification experiment, which considers all of the DR degrees as the same class. The other one is Kaggle Chest X-Ray [24] dataset on the pneumonia classification task, which consists of 5,863 X-Ray images labeled with ‘Pneumonia’ or ‘Normal’.

Pretrained diagnosis network. We choose the ResNet-50 [20] and VGG-16 [49] models pretrained using ImageNet as diagnosis network. All images are resized to $128 \times 128 \times 3$ and normalized to $[0,1]$. The models are trained with augmented data using random crop and horizontal flip. All of the models achieve high area under curve (AUC) scores on both the Fundoscopy and the Chest X-Ray datasets: ResNet-50 reaches 98.7% and 96.5%, while VGG-16 reaches 97.8% and 95.2%, respectively.

Adversarial detectors. In experiments, we choose kernel density (KD) [16], local intrinsic dimensionality (LID) [33], Mahalanobis distance (MAHA) [26], and deep neural net-

work (DNN) [37] as our baselines. The parameters for KD, LID and MAHA are set per original papers. Differently, we compute the anomaly scores of KD, LID and MAHA for all of the activation layers and summarize the anomaly scores as the final score. For DNN, we train a classifier for each activation layer and embed these networks by summing up their logits.

Adversarial attacks. For conventional attacks, we select fast gradient sign method (FGSM) [18], basic iterative method (BIM) [25], momentum iterative method (MIM) [11], projected gradient descent (PGD) [35], diverse input method (BIM) [25], translation-invariant method (TIM) [12] and Carlini and Wagner (CW) [4]. Furthermore, we choose transfer attack (TF) [31] which uses VGG-16 [49] as the substitute network. Here we choose $L_\infty = 16/256$ and $L_2 = 8/256$ as the constraints.

We choose three adaptive attacks, which imitate the clean features while manipulating the prediction: 1) Feature attack (Fea) [47], which generates adversarial features equal to a natural one. 2) Hierarchical feature constraint (HFC) [58], which pushes adversarial features toward the normal distribution of the targeted class. 3) White-box attack (WBA), we assume the attacker can access the parameters of the “shield” and directly reduce $S_y[f_\theta(C_\lambda(\hat{x}_m^*))]$ by optimizing the following object function:

$$J_{wba} = S_\phi[f_\theta(C_\lambda(\hat{x}_s^*))] + J_{cw} \quad (9)$$

All of the adaptive attacks generate stronger perturbations under $L_\infty = 16/256$ by iteratively optimizing the object function with 100 steps with random initialization. Furthermore, we strengthen the WB attack by decaying the step size [6] in each iteration with factor 10 after the 50 steps, marked as (WB_d).

Metrics. We choose two metrics to evaluate the effectiveness of the adversarial detectors: 1) *True positive rate at 90% true negative rate (TPR@90)*: The detector will drop 10% of the normal samples to reject more adversarial at-

tacks; 2) *Area under curve (AUC) score*.

Training details. We set JPEG compression with $\lambda = 80$ quality as “Cushion”. The detectors in “Shield” extract features from the $[1^{st}, 4^{th}, 8^{th}, 14^{th}]$ residual block in ResNet-50 and the $[3^{rd}, 6^{th}, 9^{th}, 12^{th}]$ activation layer in VGG-16. For the adversarial detectors, we choose ResNet-50 as backbone, and inject the feature $f_{\theta}(C_{\lambda}(x))$ into the detector by a convolutional layer with 1×1 kernel. To stably train the “Shield”, we increase the perturbation constraint of adversarial examples from $L_{\infty} = 1/256$ to $L_{\infty} = 16/256$ in each epoch, with 25 epochs in total.

4.2. Effectiveness of “Cushion”

We first reproduce the combat between the state-of-the-art adversarial detectors against the adaptive attack using HFC [58]. As shown in Table 2, the attacker can easily utilize hierarchical feature constraint to mimic the clean features and herein bypass these detectors. However, after deploying “Cushion” as a preprocessing step, the ability of the adversarial examples to manipulate deep representations is limited (even equipped with BPDA [2]). As a result, the bypassed detector can reject some of the adversarial examples with the help of “Cushion”. The results in Table 2 confirm that “Cushion” significantly improves the detectors’ performances, e.g., the AUROC score of MAHA is improved from 0 to about 80 regardless the attack method. Especially, with the help of “Cushion”, our Medical Aegis defeats HFC completely with 100% accuracy.

4.3. Effectiveness of “Medical Aegis”

To evaluate the ability of our method to defeat the notorious adversarial attacks, we use “Shield” and “Medical Aegis” to defend different backbones (ResNet-50 [20] and VGG-16 [49]) on different datasets (Fundoscopy and Chest X-Ray) against various state-of-the-art conventional attacks (in Table 3) and strong adaptive attacks (in Table 4).

The experimental results show that the “Shield” can protect the diagnosis network with AUC scores larger than 95%. Even the attacker can access all of the strategies and parameters of the detectors, the “Shield” can also distinguish most of adaptive examples with AUC scores larger than 90%, which **greatly exceeds** other detectors evaluated in Table 2. The fact proves that some unique characteristics of the notorious attacks have been captured by the “Shield” after adversarial training in the feature space. Surprisingly, when the “Medical Aegis” weakens the attacker with the “Cushion”, **nearly all of the adversarial attacks with great perturbation budget** can not defeat our defense, despite the attacker tries to bypass the “Cushion” with BPDA [2] and directly reduces the logit $S_y[f_{\theta}(C_{\lambda}(\hat{x}_m^*))]$ of the Shield by optimizing Eq. 9.

However, there is a performance drop when detecting adversarial examples generated by CW attack on the Fun-

doscopy dataset. We discuss this limitation in Section 4.4.

Table 4. The performances of “Shield” and “Medical Aegis” against three **adaptive attacks** on different datasets and backbones. When we deploy “Cushion” as a pre-processing step, the adversarial attack will automatically equip BPDA [2]. The adversarial examples are under the constrain $L_{\infty} = 16/256$. We use AUC score (%) as the metric.

Fundoscopy	Defends	Fea	HFC	WB	WB _d
ResNet-50	Shield	97.6	97.7	90.6	92.5
	Medical Aegis	100	99.9	99.1	98.7
VGG-16	Shield	97.5	98.5	92.0	92.5
	Medical Aegis	100	100	100	100
Chest X-Ray	Defends	Fea	HFC	WB	WB _d
ResNet-50	Shield	97.8	96.8	90.2	92.7
	Medical Aegis	100	100	100	100
VGG-16	Shield	98.8	99.0	91.0	91.8
	Medical Aegis	100	100	99.7	99.7

4.4. Ablation study

Shallow vs deep features. Based on the finding confirmed in Table 1 that attacker has less ability to manipulate shallow features than deep ones, we hypothesize that *adaptive attacks may leave more trails in shallow features than in deep one*. To explore which layer offers more help to the “Shield” in identifying the notarial attacks, we separately extract features from the $[3^{rd}, 6^{th}, 9^{th}, 12^{th}]$ activation layer of the pretrained VGG-16 and train a new “Shield” respectively.

As shown in Table 5, the features from a shallow layer (the $[3^{rd}$ or $6^{th}]$ layer) contribute most of the performances, while the detector only trained on the features from a deep layer (the $[9^{th}$ or $12^{th}]$ layer) is completely defeated by the adaptive attacks. This result exactly confirms our conjecture above. Therefore, it is encouraged to detect adaptive attacks in the shallow layers instead of deep ones. In addition, extracting features from multiple layers help the “Shield” achieve the best performances.

The choice of “Cushion”. We choose different denoising approaches as “Cushions”, such as JPEG compression [15] with different quality (we choose 70, 80, 90 in this paper), Bit compression (we clip the last 3 and 4 bits respectively) and total variation minimization (TVM) [19]. The performance shown in Table 6 validates that all of the denoising blocks are able to help the “Shield” defend the adaptive attacks with nearly 100% accuracy. At the same time, using these “Cushions” affects the performance of the diagnosis network slightly.

Use different perturbation budgets. In this section, we train “Medical Aegis” using the adversarial examples under different perturbation budgets, and evaluate their performances against the white-box adaptive attack (WB) under different constraints. The results shown in Table 7

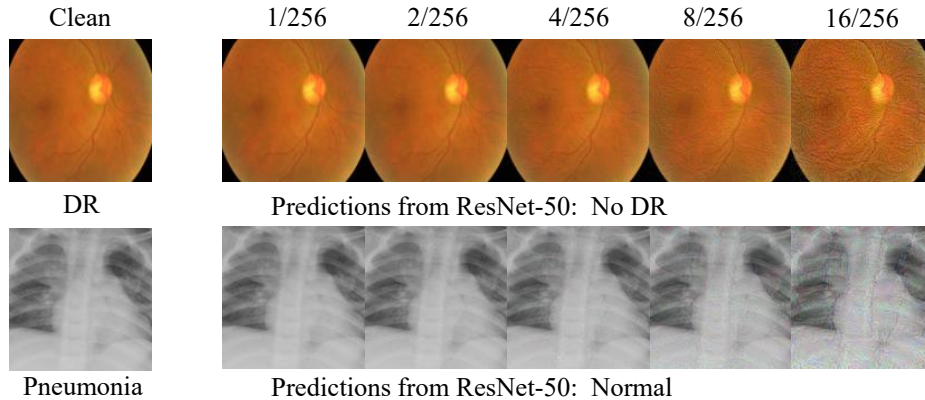


Figure 2. The visualization of the adversarial examples generated by PGD [35] under then constraint from $L_\infty = 1/256$ to $L_\infty = 16/256$.

Table 5. Comparison of the performances using the features from different layers of VGG-16. All of the attacks are under constraint $L_\infty = 16/256$ on the Fundoscopy dataset. We use AUC score (%) as the metric.

Layer Index				PGD	CW	HFC	WB
3	6	9	12				
✓	✓	✓	✓	100	93.6	100	100
✓	×	×	×	100	87.6	100	99.9
×	✓	×	×	100	87.5	99.9	97.8
×	×	✓	×	84.1	86.2	86.8	36.2
×	×	×	✓	100	77.2	76.3	41.9

Table 6. Comparison of the performances of “Medical Aegis” using different denoising methods as “Cushion”. All of the attacks are under constraint $L_\infty = 16/256$ on the Fundoscopy dataset. We use the AUC score (%) as the metric. We use VGG-16 as the backbone. We also report the performance (of the disease classification) of the diagnosis networks (Model) after applying “Cushion”.

Cushions	Model	PGD	Fea	HFC	WB
No “Cushion”	99.7	99.7	97.7	97.7	92.0
JPEG-90	99.7	100	100	100	99.6
JPEG-80	99.6	100	100	100	100
JPEG-70	99.1	100	99.1	100	100
Bit-3	99.3	100	100	100	99.3
Bit-4	96.8	100	100	100	100
TVM	99.2	100	100	100	100

show that the detector trained with small perturbations ($L_\infty \leq 4/256$) can not defeat the adaptive attack using large perturbations. However, “Medical Aegis” trained by the adversarial example with large perturbation budgets loses some ability to reject the WB attack, as well as the CW Attack on the Fundoscopy dataset (as shown in Table 3). We guess that the “Medical Aegis” may overfit on the adversarial examples with large perturbations, which is a limitation of our work and a future work direction.

Table 7. Comparison of the performances of the “Medical Aegis” trained on the adversarial examples with different perturbation budgets (each row of the table represents a model trained with $L_\infty = \rho/256$). We evaluate the model against the white-box adaptive attack (WB) under different $L_\infty = \epsilon/256$ constraints. We use the AUC score (%) as the metric. We use VGG-16 as the backbone.

Fundoscopy	$\epsilon = 2$	$\epsilon = 4$	$\epsilon = 8$	$\epsilon = 16$
$\rho = 2$	95.6	61.7	15.6	0.0
$\rho = 4$	97.5	99.7	61.5	12.5
$\rho = 8$	92.7	99.4	100	100
$\rho = 16$	85.0	98.0	100	100

5. Conclusion

We propose “Medical Aegis”, a robust adversarial defense system against an array of strong adversarial attacks, especially for the adaptive attack. “Medical Aegis” aggregates the advantages of the proactive and reactive defenses for the first time, which consists of two parts: (i) a “Cushion” module to remove the high-frequent component of the input image, which effectively weaken the attacker’s ability to manipulate the medical features; and (ii) a “Shield” module that is trained to capture the trails left by the adversarial attack in latent feature space, especially the shallow layers.

Abundant experiments on two representative public medical disease diagnosis datasets and different backbones validate the effectiveness of “Medical Aegis”. “Cushion” greatly improves the existing adversarial detectors’ performance against the adaptive attack by preventing the attacker from arbitrarily manipulating the medical features. Further, “Shield” together with “Cushion” successfully defeats most of the adversarial examples with high accuracy, including the strongest adaptive attack. In the future, we plan to improve the generalization of “Medical Aegis” on the adversarial examples with different perturbation budgets.

References

- [1] Ahmed Abusnaina, Yuhang Wu, Sunpreet Arora, Yizhen Wang, Fei Wang, Hao Yang, and David Mohaisen. Adversarial example detection using latent neighborhood graph. In *Proceedings of the IEEE/CVF International Conference on Computer Vision (ICCV)*, pages 7687–7696, October 2021. 3
- [2] Anish Athalye, Nicholas Carlini, and David Wagner. Obfuscated gradients give a false sense of security: Circumventing defenses to adversarial examples. In *International Conference on Learning Representations*, 2018. 1, 3, 4, 5, 6, 7
- [3] Nicholas Carlini and David Wagner. Adversarial examples are not easily detected: Bypassing ten detection methods. In *Proceedings of the 10th ACM Workshop on Artificial Intelligence and Security*, pages 3–14, 2017. 1, 3
- [4] Nicholas Carlini and David Wagner. Towards evaluating the robustness of neural networks. In *IEEE Symposium on Security and Privacy*, pages 39–57, 2017. 3, 6
- [5] Gilad Cohen, Guillermo Sapiro, and Raja Giryes. Detecting adversarial samples using influence functions and nearest neighbors. In *IEEE/CVF Conference on Computer Vision and Pattern Recognition*, pages 14453–14462, 2020. 2, 3
- [6] Francesco Croce and Matthias Hein. Reliable evaluation of adversarial robustness with an ensemble of diverse parameter-free attacks. In *International conference on machine learning*, pages 2206–2216. PMLR, 2020. 6
- [7] Laura Daza, Juan C Pérez, and Pablo Arbeláez. Towards robust general medical image segmentation. In *MICCAI*, pages 3–13. Springer, 2021. 1
- [8] Zhijie Deng, Xiao Yang, Shizhen Xu, Hang Su, and Jun Zhu. Libre: A practical bayesian approach to adversarial detection. In *Proceedings of the IEEE/CVF Conference on Computer Vision and Pattern Recognition*, pages 972–982, 2021. 2, 3
- [9] Guneet S Dhillon, Kamyar Azizzadenesheli, Zachary C Lipton, Jeremy Bernstein, Jean Kossaiji, Aran Khanna, and Anima Anandkumar. Stochastic activation pruning for robust adversarial defense. In *International Conference on Learning Representations*, 2018. 3
- [10] Yinpeng Dong, Qi-An Fu, Xiao Yang, Tianyu Pang, Hang Su, Zihao Xiao, and Jun Zhu. Benchmarking adversarial robustness. In *IEEE/CVF Conference on Computer Vision and Pattern Recognition*, 2020. 1, 3
- [11] Yinpeng Dong, Fangzhou Liao, Tianyu Pang, Hang Su, Jun Zhu, Xiaolin Hu, and Jianguo Li. Boosting adversarial attacks with momentum. In *IEEE/CVF Conference on Computer Vision and Pattern Recognition*, pages 9185–9193, 2018. 1, 3, 6
- [12] Yinpeng Dong, Tianyu Pang, Hang Su, and Jun Zhu. Evading defenses to transferable adversarial examples by translation-invariant attacks. In *Proceedings of the IEEE Computer Society Conference on Computer Vision and Pattern Recognition*, 2019. 3, 6
- [13] Ranjie Duan, Xingjun Ma, Yisen Wang, James Bailey, A. K. Qin, and Yun Yang. Adversarial camouflage: Hiding physical-world attacks with natural styles. In *IEEE/CVF Conference on Computer Vision and Pattern Recognition*, June 2020. 1
- [14] Abhimanyu Dubey, Laurens van der Maaten, Zeki Yalniz, Yixuan Li, and Dhruv Mahajan. Defense against adversarial images using web-scale nearest-neighbor search. In *IEEE/CVF Conference on Computer Vision and Pattern Recognition*, pages 8767–8776, 2019. 3
- [15] Gintare Karolina Dziugaite, Zoubin Ghahramani, and Daniel M Roy. A study of the effect of JPG compression on adversarial images. *arXiv preprint arXiv:1608.00853*, 2016. 3, 4, 7
- [16] Reuben Feinman, Ryan R Curtin, Saurabh Shintre, and Andrew B Gardner. Detecting adversarial samples from artifacts. *arXiv preprint arXiv:1703.00410*, 2017. 2, 3, 6
- [17] Samuel G Finlayson, Hyung Won Chung, Isaac S Kohane, and Andrew L Beam. Adversarial attacks against medical deep learning systems. *Science*, 363(6433):1287–1289, 2018. 1, 6
- [18] Ian J Goodfellow, Jonathon Shlens, and Christian Szegedy. Explaining and harnessing adversarial examples. In *International Conference on Learning Representations*, 2015. 3, 6
- [19] Chuan Guo, Mayank Rana, Moustapha Cisse, and Laurens Van Der Maaten. Countering adversarial images using input transformations. *arXiv preprint arXiv:1711.00117*, 2017. 1, 3, 4, 7
- [20] Kaiming He, Xiangyu Zhang, Shaoqing Ren, and Jian Sun. Deep residual learning for image recognition. In *IEEE/CVF Conference on Computer Vision and Pattern Recognition*, pages 770–778, 2016. 6, 7
- [21] Xiang He, Sibe Yang, Guanbin Li, Haofeng Li, Huiyou Chang, and Yizhou Yu. Non-local context encoder: Robust biomedical image segmentation against adversarial attacks. In *Proceedings of the AAAI Conference on Artificial Intelligence*, volume 33, pages 8417–8424, 2019. 3
- [22] Andrew Ilyas, Shibani Santurkar, Dimitris Tsipras, Logan Engstrom, Brandon Tran, and Aleksander Madry. Adversarial examples are not bugs, they are features. *Advances in Neural Information Processing Systems*, 2019. 4
- [23] Kaggle. APTOS 2019 Blindness Detection, 2019. <https://www.kaggle.com/c/aptos2019-blindness-detection>. 6
- [24] Kaggle. "Chest X-Ray Images (Pneumonia)", 2019. <https://www.kaggle.com/paultimothymooney/chest-xray-pneumonia>. 6
- [25] Alexey Kurakin, Ian Goodfellow, and Samy Bengio. Adversarial machine learning at scale. In *International Conference on Learning Representations*, 2017. 3, 4, 6
- [26] Kimin Lee, Kibok Lee, Honglak Lee, and Jinwoo Shin. A simple unified framework for detecting out-of-distribution samples and adversarial attacks. In *Advances in Neural Information Processing Systems*, pages 7167–7177, 2018. 2, 3, 6
- [27] Xin Li and Fuxin Li. Adversarial examples detection in deep networks with convolutional filter statistics. In *Proceedings of the IEEE International Conference on Computer Vision*, pages 5764–5772, 2017. 3

- [28] Xin Li and Dongxiao Zhu. Robust detection of adversarial attacks on medical images. In *IEEE International Symposium on Biomedical Imaging*, pages 1154–1158. IEEE, 2020. 2, 3
- [29] Fangzhou Liao, Ming Liang, Yinpeng Dong, Tianyu Pang, Xiaolin Hu, and Jun Zhu. Defense against adversarial attacks using high-level representation guided denoiser. In *IEEE/CVF Conference on Computer Vision and Pattern Recognition*, pages 1778–1787, 2018. 3
- [30] Xuanqing Liu, Minhao Cheng, Huan Zhang, and Cho-Jui Hsieh. Towards robust neural networks via random self-ensemble. In *Proceedings of the European Conference on Computer Vision*, pages 369–385, 2018. 3
- [31] Yanpei Liu, Xinyun Chen, Chang Liu, and Dawn Song. Delving into transferable adversarial examples and black-box attacks. In *International Conference on Learning Representations*, 2017. 6
- [32] Jiajun Lu, Theerasit Issaranon, and David Forsyth. SafetyNet: Detecting and rejecting adversarial examples robustly. In *Proceedings of the IEEE International Conference on Computer Vision*, Oct 2017. 3
- [33] Xingjun Ma, Bo Li, Yisen Wang, Sarah M Erfani, Sudanthi Wijewickrema, Grant Schoenebeck, Dawn Song, Michael E Houle, and James Bailey. Characterizing adversarial subspaces using local intrinsic dimensionality. In *International Conference on Learning Representations*, 2018. 3, 6
- [34] Xingjun Ma, Yuhao Niu, Lin Gu, Yisen Wang, Yitian Zhao, James Bailey, and Feng Lu. Understanding adversarial attacks on deep learning based medical image analysis systems. *Pattern Recognition*, 2020. 2, 3, 6
- [35] Aleksander Madry, Aleksandar Makelov, Ludwig Schmidt, Dimitris Tsipras, and Adrian Vladu. Towards deep learning models resistant to adversarial attacks. In *International Conference on Learning Representations*, 2018. 3, 4, 5, 6, 8
- [36] Dongyu Meng and Hao Chen. MagNet: a two-pronged defense against adversarial examples. In *Proceedings of the 2017 ACM SIGSAC Conference on Computer and Communications Security*, pages 135–147, 2017. 3
- [37] Jan Hendrik Metzen, Tim Genewein, Volker Fischer, and Bastian Bischoff. On detecting adversarial perturbations. In *International Conference on Learning Representations*, 2017. 3, 6
- [38] David J Miller, Zhen Xiang, and George Kesidis. Adversarial learning targeting deep neural network classification: A comprehensive review of defenses against attacks. *Proceedings of the IEEE*, 108(3):402–433, 2020. 3
- [39] Seyed-Mohsen Moosavi-Dezfooli, Alhussein Fawzi, and Pascal Frossard. DeepFool: a simple and accurate method to fool deep neural networks. In *IEEE/CVF Conference on Computer Vision and Pattern Recognition*, pages 2574–2582, 2016. 3
- [40] Utku Ozbulak, Arnout Van Messem, and Wesley De Neve. Impact of adversarial examples on deep learning models for biomedical image segmentation. In *Medical Image Computing and Computer Assisted Intervention*, pages 300–308. Springer, 2019. 1
- [41] Nicolas Papernot and Patrick McDaniel. Deep k-nearest neighbors: Towards confident, interpretable and robust deep learning. *arXiv preprint arXiv:1803.04765*, 2018. 3
- [42] Nicolas Papernot, Patrick McDaniel, Ian Goodfellow, Somesh Jha, Z Berkay Celik, and Ananthram Swami. Practical black-box attacks against machine learning. In *ASIA Computer and Communications Security*, pages 506–519, 2017. 3
- [43] Nicolas Papernot, Patrick McDaniel, Xi Wu, Somesh Jha, and Ananthram Swami. Distillation as a defense to adversarial perturbations against deep neural networks. In *IEEE Symposium on Security and Privacy*, pages 582–597. IEEE, 2016. 3
- [44] Omkar M Parkhi, Andrea Vedaldi, and Andrew Zisserman. Deep face recognition. In *British Machine Vision Conference*, 2015. 1
- [45] Magdalini Paschali, Sailesh Conjeti, Fernando Navarro, and Nassir Navab. Generalizability vs. robustness: investigating medical imaging networks using adversarial examples. In *Medical Image Computing and Computer Assisted Intervention*, pages 493–501. Springer, 2018. 1
- [46] Andrew Slavin Ross and Finale Doshi-Velez. Improving the adversarial robustness and interpretability of deep neural networks by regularizing their input gradients. In *Proceedings of the AAAI Conference on Artificial Intelligence*, 2017. 3
- [47] Sara Sabour, Yanshuai Cao, Fartash Faghri, and David J Fleet. Adversarial manipulation of deep representations. In *IEEE Symposium on Security and Privacy*, 2016. 3, 6
- [48] Ali Shafahi, Mahyar Najibi, Amin Ghiasi, Zheng Xu, John Dickerson, Christoph Studer, Larry S Davis, Gavin Taylor, and Tom Goldstein. Adversarial training for free! *Advances in Neural Information Processing Systems*, 2019. 1, 3
- [49] Karen Simonyan and Andrew Zisserman. Very deep convolutional networks for large-scale image recognition. In *International Conference on Learning Representations*, 2015. 6, 7
- [50] Christian Szegedy, Wojciech Zaremba, Ilya Sutskever, Joan Bruna, Dumitru Erhan, Ian Goodfellow, and Rob Fergus. Intriguing properties of neural networks. In *International Conference on Learning Representations*, 2014. 1
- [51] Saeid Asgari Taghanaki, Kumar Abhishek, Shekoofeh Azizi, and Ghassan Hamarneh. A kernelized manifold mapping to diminish the effect of adversarial perturbations. In *IEEE/CVF Conference on Computer Vision and Pattern Recognition*, pages 11340–11349, 2019. 3
- [52] Florian Tramer, Nicholas Carlini, Wieland Brendel, and Aleksander Madry. On adaptive attacks to adversarial example defenses. In *Advances in Neural Information Processing Systems*, 2020. 1, 3
- [53] Florian Tramèr, Alexey Kurakin, Nicolas Papernot, Ian Goodfellow, Dan Boneh, and Patrick McDaniel. Ensemble adversarial training: Attacks and defenses. In *International Conference on Learning Representations*, 2018. 1, 3
- [54] Dimitris Tsipras, Shibani Santurkar, Logan Engstrom, Alexander Turner, and Aleksander Madry. Robustness may be at odds with accuracy. *International Conference on Learning Representations*, 2019. 1, 3

- [55] Cihang Xie, Zhishuai Zhang, Yuyin Zhou, Song Bai, Jianyu Wang, Zhou Ren, and Alan L Yuille. Improving transferability of adversarial examples with input diversity. In *Proceedings of the IEEE/CVF Conference on Computer Vision and Pattern Recognition*, pages 2730–2739, 2019. [3](#)
- [56] Weilin Xu, David Evans, and Yanjun Qi. Feature squeezing: Detecting adversarial examples in deep neural networks. In *Network and Distributed System Security Symposium*, 2017. [3](#)
- [57] Qingsong Yao, Zecheng He, Hu Han, and S Kevin Zhou. Miss the point: Targeted adversarial attack on multiple landmark detection. In *Medical Image Computing and Computer Assisted Intervention*, pages 692–702. Springer, 2020. [1](#), [2](#)
- [58] Qingsong Yao, Zecheng He, Yi Lin, Kai Ma, Yefeng Zheng, and S Kevin Zhou. A hierarchical feature constraint to camouflage medical adversarial attacks. *Medical Image Computing and Computer Assisted Intervention*, 2021. [2](#), [3](#), [6](#), [7](#)
- [59] Xuwang Yin, Soheil Kolouri, and Gustavo K Rohde. Gat: Generative adversarial training for adversarial example detection and robust classification. In *International Conference on Learning Representations*, 2020. [2](#)
- [60] Zhihao Zheng and Pengyu Hong. Robust detection of adversarial attacks by modeling the intrinsic properties of deep neural networks. In *Advances in Neural Information Processing Systems*, pages 7913–7922, 2018. [3](#)